SUPPLEMENTARY INFORMATION

AuNPs/rGO-Enhanced Molecularly Imprinted Field-Effect Transistor Sensor for Highly Selective Detection of Lactic Acid in Sweat

Yi Xiong[a], Hong Zhu[a], Lei Wang[a], Runan Tan[a], Ting Wang[a], Ping Wang[c]*, Hanping He[b]*, Gang Chang[a]*

[a] Ministry of Education Key Laboratory for the Green Preparation and Application of Functional Materials, Hubei Key Laboratory of Polymer Materials, School of Materials Science and Engineering, Hubei University, Wuhan 430062, China

[b] College of Health Science and Engineering, Hubei University, Wuhan 430062, China

[c] Department of Clinical Laboratory, Union Hospital, Tongji Medical College, Huazhong University of Science and Technology, Wuhan 430022, China

Corresponding author e-mail: 2000xh0689@hust.edu.cn; hehanping@hubu.edu.cn; changgang@hubu.edu.cn

Contents

reported LA sensors.

T3. Real Sample Analysis.

T4. Comparison of the proposed sensor with a commercial lactate assay kit for LA detection in sweat samples.

Figure. S1

FE-SEM image of interdigitated finger electrodes with Al_2O_3 ceramic substrate.

Figure. S2

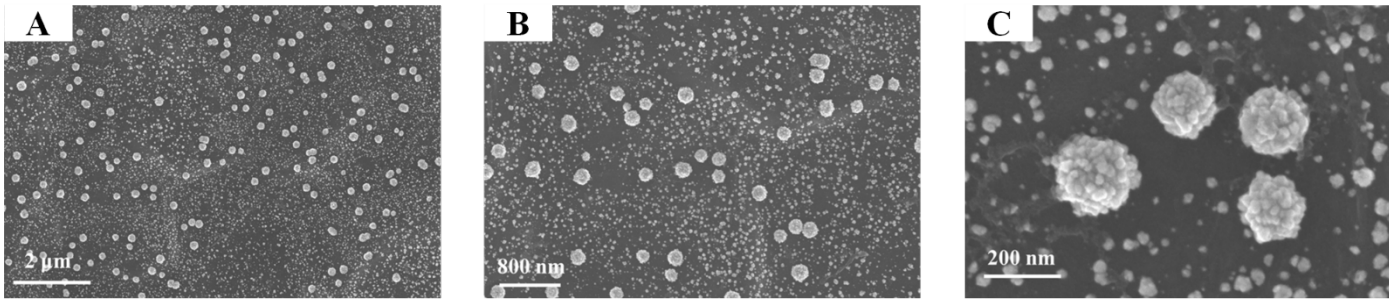

SEM image of AuNPs electrodeposited on the rGO surface at - 0.40 V with a deposition time exceeding 70 s.

Figure. S3

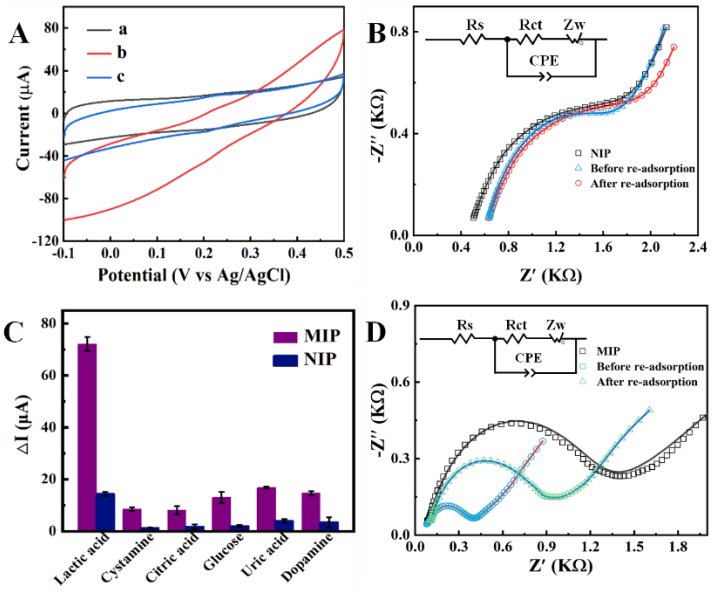

(A) CV and (B) Nyquist plots of NIP/AuNPs/rGO-GCE. (C) Selectivity comparison between MIP/AuNPs/rGO-GCE and NIP/AuNPs/rGO-GCE sensors toward LA and various interferents. (D) Nyquist plots of MIP/AuNPs/rGO-GCE before template elution, after template elution, and after LA rebinding in 5 mM $[Fe(CN)_6]^{3-/4-}$ solution. Solid lines represent fits to the equivalent circuit model. Fitted parameters with 95% confidence intervals are summarized in the tables below.

Table (B): Fitted EIS parameters for NIP/AuNPs/rGO-GCE before template elution, after template elution, and after LA rebinding in 5 mM $[Fe(CN)_6]^{3-/4-}$ solution.

contents	R_s (Ω)	R_{ct} (Ω)	CPE-P (n)	CPE-T (Y_0)	W_R	W_P	χ^2
NIP	579.5±2.58	1671±36.98	0.63±0.006	$1.18\times10^{-5}\pm5.75\times10^{-7}$	2678±26.12	0.66±0.020	1.26×10^{-4}
Before adsorption	452.6±6.93	1554±724.16	0.64±0.040	$1.12\times10^{-5}\pm4.33\times10^{-6}$	336±18.03	0.35±0.009	2.69×10^{-4}
After adsorption	582.5±6.25	1563±76.03	0.64±0.016	$1.60\times10^{-5}\pm1.88\times10^{-6}$	4635±45.55	0.79±0.054	1.60×10^{-3}

Table (D): Fitted EIS parameters for MIP/AuNPs/rGO-GCE before template elution, after template elution, and after LA rebinding in 5 mM $[Fe(CN)_6]^{3-/4-}$ solution.

contents	R_s (Ω)	R_{ct} (Ω)	CPE-P (n)	CPE-T (Y_0)	W_R	W_P	χ^2
MIP	72.02±1.56	1092±40.18	0.80±0.007	$4.60\times10^{-6}\pm2.95\times10^{-7}$	5215±81.94	0.32±0.024	1.89×10^{-3}
Before adsorption	56.4±2.32	319.2±13.49	0.73±0.018	$9.04\times10^{-6}\pm1.40\times10^{-6}$	2153±111.8	0.41±0.019	3.18×10^{-4}
After adsorption	84.09±1.91	768.5±20.04	0.79±0.010	$5.71\times10^{-6}\pm4.65\times10^{-7}$	3447±302.03	0.38±0.023	2.40×10^{-3}

Note: All values are mean ± 95% confidence intervals (standard error × 1.96).

Figure. S4

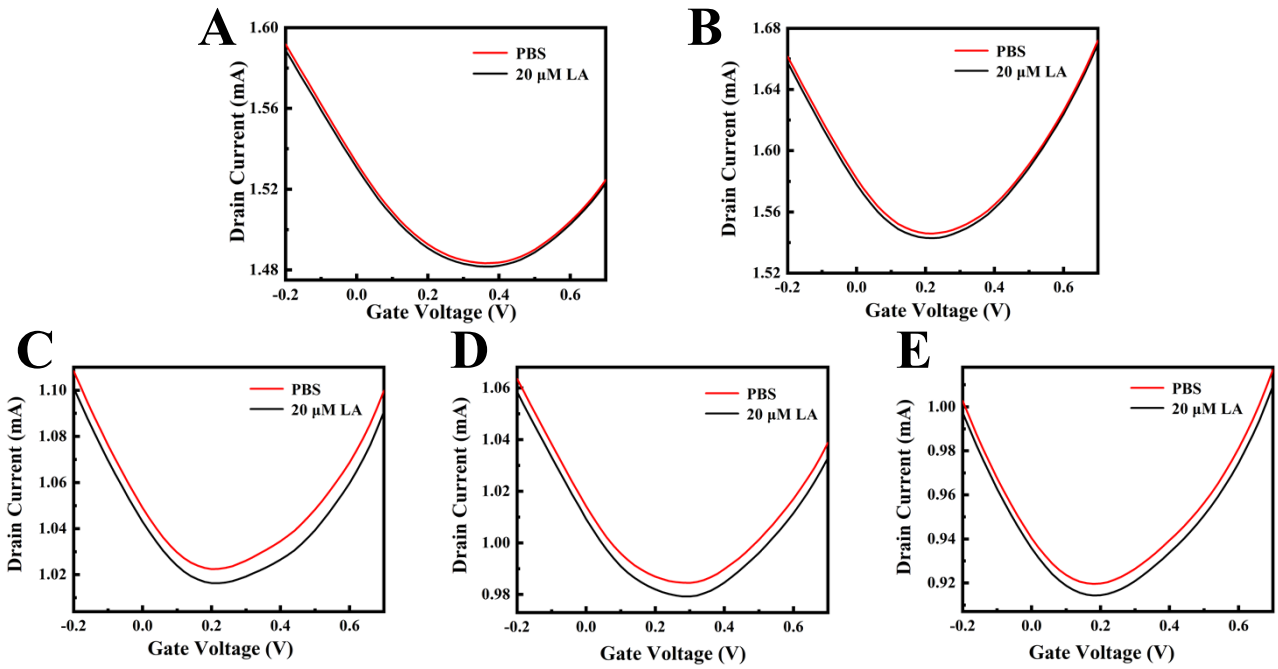

Transfer curves of MIP/AuNPs/rGO-FET in the presence of 20 μM LA at o-PD to LA molar ratios of (A) 2.5:1, (B) 5:1, (C) 10:1, (D) 20:1, and (E) 40:1.

Figure. S5

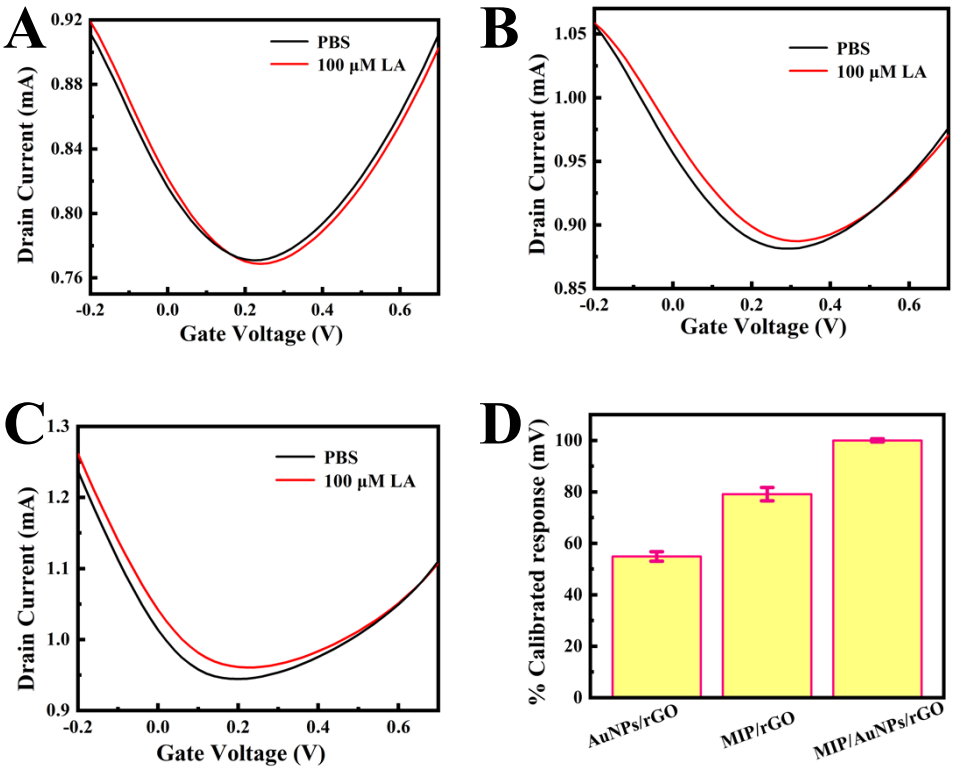

Transfer curves of (A) AuNPs/rGO-FET, (B) MIP/rGO-FET, and (C) MIP/AuNPs/rGO-FET upon exposure to 100 μM LA after template elution. (D) Comparison of voltage response values (ΔV) for different device configurations to 100 μM LA.

Figure. S6

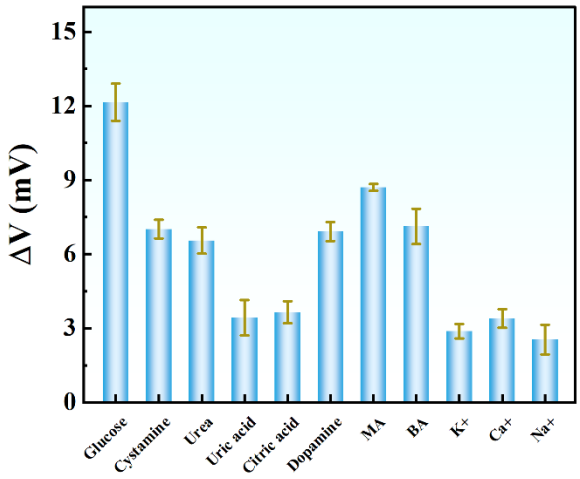

Selectivity of the MIP/AuNPs/rGO-FET sensor for LA in the presence of 10 mM common sweat interferents.

Figure. S7

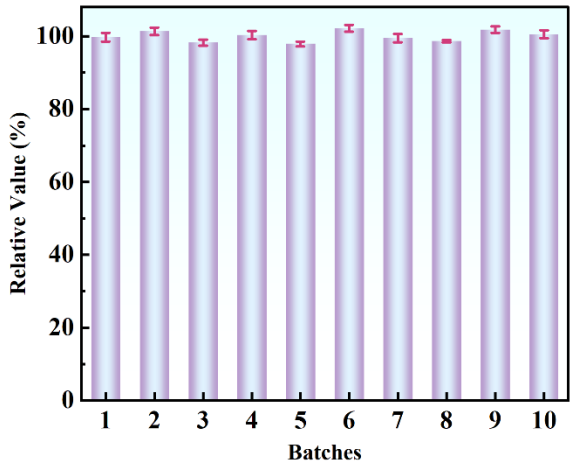

Comparison of performance between multiple batches of MIP/AuNPs/rGO-FET sensors.

Table. S1 Statistical analysis of performance metrics for ten independent MIP/AuNPs/rGO-FET sensors.

Sample (No.)	V_{Dirac} (V)	g_m (mS)	I_{ds} (mA)	μ (cm^2 /(V·s))
1	0.18	1.013	1.2319	6.26
2	0.18	0.9897	1.2363	6.12
3	0.18	0.9777	1.2380	6.05
4	0.18	0.9502	1.2383	5.88
5	0.16	0.9619	1.2342	5.95
6	0.16	0.9496	1.2358	5.87
7	0.16	0.9411	1.2360	5.82
8	0.16	0.9682	1.2354	5.99
9	0.16	0.9496	1.2358	5.87
10	0.16	0.9532	1.2367	5.90
Mean value	0.168	0.965	1.238	5.97
RSD (%)	1.03	2.2	0.42	13.7

Table. S2 Comparison of analytical performance of MIP/AuNPs/rGO-FET with previously reported LA sensors.

Material	Method	LOD	Linear range	Ref.
MIP/AuNPs/rGO-GCE	CV	89.3 pM	0.1 nM-15 nM	[1]
MIP	UV-Vis	0.162 mM	0.1 mM-1.7 mM	[2]
MIP/AgNWs	DPV	0.22 μM	1 μM-0.1 M	[3]
MIP/rGO/AgNPs/AuE	CV	0.72 μM	10 μM-50 μM	[4]
Nafion/ LOx	OECT	100 pM	100 pM-10 mM	[5]
Nafion-LOx/PPy/MWCNT/PA6	OECT	1 nM	1 nM-1 mM	[6]
LDH/Chit	NiO FET	0.2 aM	1 aM-1 pM	[7]
AlGaAs/GaAs	ZnONWs FET	30 pM	30 pM-300 mM	[8]
LOx/BSA	OECT	11 nM	0.25 mM-5 mM	[9]
Ni/Al LDH	OECT	40 μM	100 mM-2.5 mM	[10]
LOx/GA-CN/HRP-OsRP/Au	EG-OFET	66 nM	60 nM-220 nM	[11]
LOx-HRP/OsRP	F-OFET	-	0 - 10 mM	[12]
PSS/MWCNTs/cotton fiber	Fb-OECT	0.28 μM	1 μM -20 mM	[13]
MIP/AuNPs/rGO-FET	FET	3.33 pM	10 pM-1 mM	This work

Notes: LOD: limit of detection; GCE: glassy carbon electrode; rGO: reduced graphene oxide; MIP: molecular imprinting layer; AuNPs: gold nanoparticle; AgNWs: silver nanowires; AgNPs: silver nanoparticles; AuE: gold electrode; LOx: lactate oxidase; PPy: polypyrrole; MWCNT: multi-walled carbon nanotubes; PA6: polyamide 6; Ni/Al LDH: Ni/Al layered double hydroxide; Chit: chitosan and BSA stands for bovine serum protein; OECT: Organic Electrochemical Transistor; EG-OFET: Extended-Gate Organic Field-Effect Transistor; F-OFET: Flexible Organic Field-Effect Transistor; HRP: Horseradish Peroxidase; OsRP: Osmium Redox Polymer; GA-CN: Glutaraldehyde Crosslinked Network; Fb-OECT: Fiber-based Organic Electrochemical Transistor; PSS: Poly(sodium 4-styrenesulfonate).

Table. S3 Real Sample Analysis.

Sample	Added	Detection	Recovery (%)	RSD (%)
Diluted Lactate sample	1 nM	1.085 nM	108.47	11.06
	100 nM	98.36 nM	98.36	9.88
	10 μM	9.886 μM	98.86	5.82
Sweat	1 nM	1.049 nM	104.93	11.30
	100 nM	101.93 nM	101.93	10.45
	10 μM	10.259 μM	102.59	7.40

Table. S4 Comparison of the proposed sensor with a commercial lactate assay kit for LA detection in sweat samples.

Sample	Number	Lactate Assay Kit (μM)	FET Detection (μM)	RD (%)	RSD (%)
Sweat	1	175	181	96.7%	1.34
	2	556	548	101.5%	2.89
	3	953	946	100.7%	1.66

References

1. T. C. Pereira and N. R. Stradiotto, Microchimica Acta, 2019, 186, 764.
2. Y. L. Mustafa and H. S. Leese, ACS Omega, 2023, 8, 8732-8742.
3. Q. Zhang, D. Jiang, C. Xu, Y. Ge, X. Liu, Q. Wei, L. Huang, X. Ren, C. Wang and Y. Wang, Sensors and Actuators B: Chemical, 2020, 320, 128325.
4. F. Ben Moussa, F. Achi, H. Meskher, A. Henni and H. Belkhalfa, Materials Chemistry and Physics, 2022, 289, 126456.
5. Y. Tao, R. Zhu, P. Hao, W. Jiang, M. Li, Q. Liu, L. Yang, Y. Wang and D. Wang, Materials Science and Engineering: B, 2023, 290, 116356.
6. Y. Zhang, Y. Wang, X. Qing, Y. Wang, W. Zhong, W. Wang, Y. Chen, Q. Liu, M. Li and D. Wang, Analytical and Bioanalytical Chemistry, 2020, 412, 7515-7524.
7. S. Mansouri Majd, A. Salimi and B. Astinchap, Biosensors and Bioelectronics, 2017, 92, 733-740.
8. S. Ma, Q. Liao, H. Liu, Y. Song, P. Li, Y. Huang and Y. Zhang, Nanoscale, 2012, 4, 6415-6418.
9. L. J. Currano, F. C. Sage, M. Hagedon, L. Hamilton, J. Patrone and K. Gerasopoulos, Scientific Reports, 2018, 8, 15890.
10. I. Gualandi, M. Tessarolo, F. Mariani, D. Arcangeli, L. Possanzini, D. Tonelli, B. Fraboni and E. Scavetta, Sensors, 2020, 20,3453.
11. T. Minami, T. Sato, T. Minamiki, K. Fukuda, D. Kumaki and S. Tokito, Biosensors and Bioelectronics, 2015, 74, 45-48.
12. T. Minamiki, S. Tokito and T. Minami, Anal Sci, 2019, 35, 103-106.
13. J. Li, Y. Fu, D. Luo, P. Li, H. Sun, T. Wang, G. Wang, L. Chen, L. Liu and H. Liu, Microchemical Journal, 2025, 219, 116170.